ELSEVIER

NeuroImage

www.elsevier.com/locate/ynimg
NeuroImage 32 (2006) 1365 – 1374

Slab-like functional architecture of higher order cortical area 21a showing oblique effect of orientation preference in the cat

Luoxiu Huang,[a] Tiande Shou,[a,b,*] Xin Chen,[a] Hongbo Yu,[a] Chao Sun,[a] and Zhiyin Liang[a]

[a] *Vision Research Lab, Center for Brain Science Research, School of Life Sciences, Fudan University, Shanghai 200433, PR China*
[b] *State Key Laboratory of Brain and Cognitive Science, Institute of Biophysics, Chinese Academy of Sciences, Beijing 100101, PR China*

Received 2 December 2005; revised 30 April 2006; accepted 3 May 2006
Available online 22 June 2006

Optical imaging based on intrinsic signals is a powerful tool for in vivo studying functional organization of various cortices. Here, the functional architecture of orientation-sensitive neurons in higher order extrastriate cortical area 21a was investigated in cats using optical imaging combined with electrophysiological methods. It is found that neurons in area 21 with similar preferred orientations were functionally organized into a slab-like columnar structure orthogonal to the cortical surface, and the orientation columns were distributed more densely than those in area 17. The responsiveness and activated areas of optical maps visually elicited by the horizontal and vertical gratings were always larger than those by oblique gratings in areas 21a and 17. This neural oblique effect shown in orientation maps was more significant in area 21a than that in area 17. The findings suggest a neuronal mechanism in the higher order extrastriate cortex involving the visual perceptive process of the superiority of cardinal contours.

Keywords: Oblique effect; Orientation column; Extrastriate cortex; Visual cortex

Introduction

For more than six decades, a huge amount of knowledge on brain function was gained from studies using electrophysiological methods including single-unit extra- and intra-cellular recordings, EEG and evoked potential recordings etc. These methods are not sufficient for getting a three-dimensional (3D) functional architecture of the brain. It was Hubel and Wiesel who used 2-deoxygglucose autoradiography technique for the first time to show the 3D deoxyglucose maps of orientation column and ocular dominance columns in monkeys (Hubel and Wiesel, 1974). However, study using the 2-deoxglucose technique requires a long time (several tens of minutes or hours) to show functional organization at a certain stimulus condition after the animal is executed. Optical imaging based on intrinsic signals is a powerful tool to in vivo study functional organization of visual cortices due to its higher spatial resolution (tens micrometers), close correlation of neuronal activity (both spiking and subthreshold activity) and numerous maps for various stimuli in the same animal. Given these advantages, we used this technique to study the functional architecture of area 21a in the cat and compared with that of area 17.

Area 21a is one of several visual cortical areas located in the middle part of caudal suprasylvian gyrus defined by anatomical connections and retinotopic organization in cats (Palmer et al., 1978; Tusa and Palmer, 1980; Tusa et al., 1981; Rosenquist, 1985; Updyke, 1986). According to Tusa and Palmer (1980, 1981), it is bounded medially and caudally by area 19 while laterally bordered by posteromedial lateral suprasylvian area (PMLS). Area 21a receives principal association inputs from the supragranular laminae of area 17 and to a lesser extent from areas 18 and 19 (Michalski et al., 1993; Montero, 1981; Grant and Shipp, 1991; Sherk and Mulligan, 1993; Dreher et al., 1996a, b) and sends extensive feedback projections to these areas in the cat (Dreher, 1986; Morley and Vickery, 1997). In its entirety, area 21a is devoted to the retinotopic representation of the central visual field within eccentricities of 20°; mainly within 5° from the area centralis of the cat's retina (Tusa and Palmer, 1980; Updyke, 1986; Wimborne and Henry, 1992).

The receptive field properties of a large majority of area 21a neurons are similar to those of neurons in area 17 in many aspects, such as having sharp orientation tuning, temporal tuning to relatively low frequencies and strong binocular interaction, however, area 21a neurons exhibit relatively lower spatial frequency tuning and larger receptive field size than those in area 17 (Dreher, 1986; Dreher et al., 1993; Tusa and Palmer, 1980; Wang et al., 2000; Wang and Dreher, 1996; Morley and Vickery, 1997). Also, the mean direction selectivity index of area 21a neurons is substantially lower than the neurons in areas 17 or 18. (Dreher et al., 1993, 1996a, b). Furthermore, unlike area 17, only the upper contralateral visual field and the strip of the retina 3–7° below the zero horizontal meridian are represented in area 21a (Dreher et al., 1993; Tusa et al., 1978;

* Corresponding author. Vision Research Lab, Center for Brain Science Research, School of Life Sciences, Fudan University, Shanghai 200433, PR China. Fax: +86 21 65643528.
E-mail address: tdshou@fudan.edu.cn (T. Shou).
Available online on ScienceDirect (www.sciencedirect.com).

1053-8119/$ - see front matter © 2006 Elsevier Inc. All rights reserved.
doi:10.1016/j.neuroimage.2006.05.007

Tusa and Palmer, 1980; Wimborne and Henry, 1992). Taken together, these similarities indicate that neurons in area 21a are mainly involved in form information processing rather than motion analysis. Besides, the orientation selective neurons in the visual cortical areas 17–19 are also arranged functionally in a columnar fashion from the pial surface to the white matter and respond preferentially to specific orientation contours in the visual world (Hubel and Wiesel, 1962, 1965, 1974). However, very little is known regarding the detailed layout of functional organization in the higher order extrastriate cortical areas, e.g., area 21a.

It is well known that visual sensitivity varies as a function of orientation, specifically human and animals show better visual acuity and responsiveness to horizontally and vertically oriented visual stimuli than to oblique ones, a phenomenon known as the oblique effect (Appelle, 1972; Howard, 1982; Campbell et al., 1966; Annis and Frost, 1973; Timmney and Muir, 1976). This psychophysical and behavioral event has been considered as a reflection of the processes of primary visual cortex (Appelle, 1972; Bonds, 1982; Howard, 1982; Shou et al., 1985; Yu and Shou, 2000; Coppola et al., 1998a, b; Furmanski and Engel, 2000; Wang et al., 2003). Thus, it is of interest to investigate whether and how the extrastriate area 21a neurons receiving mainly excitatory input from area 17 involve the oblique effect and the relationship between the effect and cortical organization. Using intrinsic signal optical imaging and electrophysiological methods, we studied the functional orientation organization of area 21a and its relation to the neural oblique effect in the cat.

Experimental procedures

Animal preparation and maintenance

Experiments were performed on 14 adult cats weighing 2.5–3.0 kg. Nine of 14 cats were employed for studying both areas 21a and 17, the remaining for area 17 only. Each cat was initially anaesthetized with ketamine HCl (20 mg/kg) i.m., and the loading dose of 4 mg/kg sodium pentobarbital was given intravenously for physiological surgery. Lidocaine HCl (1%) was given in all intended sites of surgical entry. After intravenous and tracheal cannulations were performed, cats were placed in a stereotaxic apparatus (Jiangwan II type, The Second Military Medical University, Shanghai, China). Then a mixture of sodium pentobarbital (3 mg/kg·h), gallamine triethiodide (10 mg/kg·h) and glucose (5%) in saline was infused intravenously for maintaining anesthesia and paralysis. Artificial respiration was maintained for surviving animals. The animals' physiological conditions were kept in normal ranges throughout the experiment. The end-tidal CO_2 was measured and kept at about 4% by adjusting the rate and volume of the respirator. EEG and ECG were monitored for evaluating the depth of anesthesia. The body temperature of animals was monitored and kept at 38°C. All experiments involving animals conformed to the policy of the Society for Neuroscience on the Use of Animals in Neuroscience Research.

The pupils of the cats were dilated with atropine (0.5%), and the nictitating membranes were retracted with neosynephrine (2%). The eyes were refracted carefully and corrected with appropriate contact lens; artificial pupils of 3-mm diameter were used. The eyes were focused on a tangent screen at a distance of 57 cm.

Area 21a was localized according to its relationship to the suprasylvian sulcus and to the lateral sulcus (Tusa and Palmer, 1980). The schematic and photographical figures in Fig. 1 show the location of area 21a and relative areas17, 18, 19 and PMLS. The visual cortical area 21a and area 17 were exposed at Horsley-Clarke coordinates L7–12, P1–7 and L0–8, P0–10 respectively. Special care was taken to ensure that the two optical imaging areas had concentrated on the similar and overlapped retinotopic fields using the method to measure cortical retinotopic topography elsewhere (Chen and Shou, 2003). Generally the field-of-view for areas 17 and 21a was within retinal eccentricity of 10°. Then a stainless steel chamber of 16 mm in diameter, whose large field is greatly useful for identifying the precise positions of areas 21a and 17, was cemented onto the skull surrounding the exposed areas 21a or/and 17. After careful removal of the dura, the chamber was filled with warm silicone oil and sealed with a transparent glass window. Usually optical signals were acquired respectively from areas 21a and 17 in order to get a large map of high quality even in the same experiment.

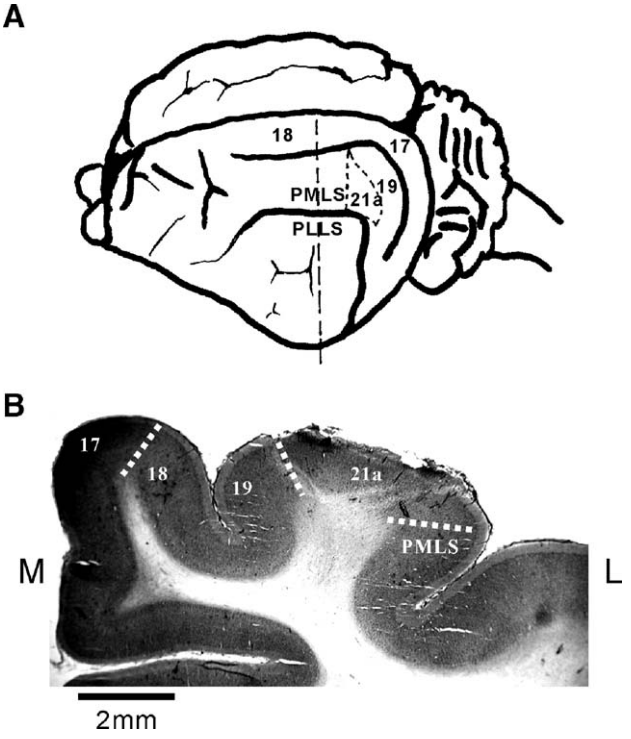

Fig. 1. Schematic figure and photographs showing the anatomical locations of area 21a and related areas in the cat's visual cortex. (A) Left lateral view of a cat's brain showing the relative location of area 21a and area 17. Numbers on the surface indicate names of various cortical areas. The area 21a is surrounded by the dotted curve. The vertical dotted line indicates the ear bar position in the Horsley–Clarke coordinates. PMLS, posteromedial lateral suprasylvian area; PLLS, posterolateral lateral suprasylvian area. (B) Coronal section of the right hemisphere showing the position of areas 21a related to areas 17, 18, 19 and PMLS. M, medial; L, lateral.

Visual stimulation

The main stimuli used in this study were computer-generated drifting sinusoidal gratings (contrast 0.9; temporal frequency 2 Hz; mean luminance 15.1 cd/m^2), and the gratings were presented on the screen of a monitor and restricted within a round area either 30° in visual angle in diameter to avoid the monitor edge-effect for optical imaging or 1° larger than a neuron's receptive field for single-unit recording. Gratings consisting of spatial frequencies

0.2–0.5 cycles/degree (c/deg) were used in all experiments due to the fact that the best orientation map of area 21a revealed by optical imaging typically appears around these spatial frequencies, in which most neurons in area 17 respond well (Moveshon et al., 1978; Wang and Dreher, 1996, Wang et al., 2000; Chen et al., 2003). A set of different orientation gratings (usually, 4 orientations equally interleaved from 0° to 180°; sometimes, 6 orientations were used for more precise measure of orientation bias of each pixel) drifting in opposite directions was used to obtain full orientation maps of the cortex in acquisition block of a computer. During the experiment differently oriented grating stimuli were randomly mixed and presented in one trial in order to decrease variation, and the time for overall data acquisition was designed to be as short as possible.

Optical imaging and electrophysiological recording

An area-scan CCD (charge-coupled device) camera (DALSA, Canada, 512 pixels × 512 pixels; 24 μm/pixel) was used to record the optical images of intrinsic signals respectively from the exposed area 21a or area 17 through the glass window of the stainless steel chamber, as reported recently (Zhan and Shou, 2002; Chen et al., 2003). A macroscope tandem lens arrangement of two coupled 50-mm lenses (f = 1:1.2) was used to achieve a very shallow depth of field (less than 100 μm) in order to alleviate the blood vessel artifacts in the functional maps, as reported elsewhere (Retzlaff and Grinvald, 1991). The vessel map on the cortical surface was obtained with green light (546 nm) shining on the surface of the cortex. Functional orientation maps of the cortical responses to grating stimuli were obtained with red light (640 nm) using the camera primarily focused at a cortical depth of 500–600 μm. Cats were stimulated binocularly by a grating presented for 2 s each. The cortical optical images of each trial were obtained from 1 s before to 2 s after the stimulating grating presentation and saved as 5 frames, each of which was for 1 s. The largest optical signals in the visual cortex always appeared 3–4 s after the onset of the stimulus (Zhan and Shou, 2002; Chen et al., 2003; Huang et al., 2004). Accordingly, only the fourth frames were chosen for further analysis. In each trial, a grating stimulus of 2 s and a blank of 10 s were presented on the screen of the display. Sixteen to sixty four repeated trials were enough to produce a clear orientation map of areas 21a or 17.

In some experiments, single neuron's activities were recorded extracellularly along a penetration orthogonal to the surface of area 21a with a micropipette electrode of 6–10 MΩ in impedance. Action potentials of single neurons were amplified and averaged by a computer. The mean firing rate of averaged poststimulus time histogram (PSTH) was defined as a cortical cell's response amplitude.

Data analysis

Data analysis was mostly performed with a data- and image-analysis program (MatLab; MathWorks, Natick, MA). First, the so-called "first frame analysis" was conducted in such a way that the first (blank image) frame was subtracted from the fourth frame in each trial in order to reduce slow wave noise. Then we averaged the treated fourth frames in all trials to eliminate random noise to get the so-called "orientation single-condition map" which refers to a functional map resulted from the difference between two images of the fourth and the first frames.

To quantify the extent of a given functional map's responsiveness, the response strength (RS) was defined and calculated. First, the "cocktail map" (i.e., the averaged map of a set of maps elicited by all different orientation stimuli for a given cortical area studied) was subtracted from a given single-condition map. Then, each the resultant map was divided by the first frame of its own map (i.e., "blank screen normalization") as a sample map, which includes all the normalized values of pixels on the map for further RS measurement of the given map. The next step included low-pass filtering using an isotropic Gaussian filter kernel whose standard deviation was equal to 2. This procedure is used to remove high-frequency noise on the map. The low-frequency noise was reduced by convolving the map with a 40 × 40 pixel mean filter kernel and by subtracting the result from it. Finally, for comparing the response strengths of different orientation maps, the averages of both the 10% maximum and the 10% minimum brightness values were respectively computed in a sample map and their difference served as a measure of the response strength (RS) of the given map. Essentially, RS represents the averaged contrast of a given orientation map which reflects the difference of responsiveness between the excited region and unexcited region of a cortical area to a visual stimulus.

To remove the high and low spatial frequency noise in the image, a band-pass filter was used. In order to display the functional map more clearly in our figures, the histogram equalization technique of MATLAB (6.0 version) was employed to enhance the contrast of a map in a nonlinear way. In detail, all the pixels in each orientation map were equally divided into 256 groups according to their brightness values. Each pixel in the brightest group was given the relative value of 256, and that in the lowest one the relative value was 1. The relative values of all pixels in the orientation map were used to produce a clearer map. In this way, the map contrast would be sharpened while keeping the visible patterns unchanged. We used this method just for better map display, not for quantitative analysis.

Two-dimensional cross-correlation coefficient (CCC) analysis was used to quantify similarity of two maps of the same cortical area obtained in different conditions pixel by pixel, as used previously (Chen et al., 2003; Godecke and Bonhoeffer, 1996). For each pair of pixels at the identically corresponding position on the two maps, the CCC was calculated from an outlined square (264 μm × 264 μm or11 pixels × 11 pixels) area around the position of the tested pair of pixels. The CCC ranges from −1.0 to 1.0 and the higher the CCC, the stronger the relationship between the two maps. Two spatially identical maps have a CCC of 1.0, and the two complementary maps a CCC of −1.0. If the two maps do not have any correlation, their CCC is zero.

We calculated the orientation preferences for each cell recorded in area 21a electrophysiologically and each pixel in a cortical orientation map optically. The statistical methods employed are described in detail in Batschelet (1981) and Zar (1974). These methods have been previously used in calculating the orientation biases of retinal ganglion cells (Levick and Thibos, 1982; Thibos and Levick, 1985), lateral geniculate nucleus (LGN) cells (Shou and Leventhal, 1989) and visual cortical cells to moving stimulus (Wörgötter and Eysel, 1987; Wörgötter et al., 1990). Briefly, the responses of each cell (or each pixel in an orientation map) to the different directions of the stimulus presented were stored in the computer as a series of vectors. The vectors were summed and divided by the sum of the absolute values of the vectors. The angle of the resultant vector gives the preferred orientation of the cell (or

the pixel). The length of the resultant vector, termed the orientation bias, provides a quantitative measure of orientation sensitivity of the cell (or the pixel here). Orientation biases ranged from 0 to 1, with 0 being completely not selective to grating orientation and 1 responding to only one orientation. Although in theory the range of orientation biases is from 0 to 1, the observed range for cortical cells was from 0 to 0.74. If the cells exhibited orientation bias >0.1, they were classified as orientation-sensitive neurons. This is a conservative criterion because the statistical methods we used indicate that a bias $\geq$0.08 is significant (Zar, 1974). Because the periodicity of orientation is 180°, the angles of the direction of the stimulus grating are multiplied by a factor of 2 when calculating orientation preference.

To estimate the orientation preference of pixels in a map, all the preferred orientations of these pixels whose orientation bias was over 0.1 were accumulated to get a color-coded polar map in which color indicates preferred orientation and brightness indicates orientation bias. Accordingly, the preferred orientation histogram was obtained for areas 21a and 17, respectively. Based on the histogram, the activated cortical areas preferentially responding to different stimuli of orientations were grouped into horizontal (0°–22.5° and 157.5°–180°), vertical (90° ± 22.5°) and oblique (45° ± 22.5° and 135° ± 22.5°) domains and compared in given cortical regions in areas 21 and 17 where their retinotopic projections were overlapped.

Histological observation

To reconstruct the electrode tracks, one electrolytic lesion was made in each microelectrode penetration in area 21a. At the end of an electrophysiological experiment, the animals were deeply anaesthetized by an overdose of sodium pentobarbital. After perfusion with phosphate-buffered solution (PBS) and fixation with a solution of 4% paraformaldehyde, the brain was removed, the part of area 21a was frozen and sectioned in 50 μm thickness. Then the conformation of the location of the electrode recording site was determined using cresyl violet staining in reference to standard maps of visual areas of the cat cortex (Tusa and Palmer, 1980; Tusa et al., 1981; Rosenquist, 1985).

Results

Functional orientation maps of area 21a

Fig. 2 shows a set of single-condition orientation maps obtained by optical imaging based on intrinsic signals in area 21a when the cat's eye was visually stimulated in the central part of visual field with gratings of orientation 0°, 45°, 90° and 135° respectively. All the maps exhibited strip-like patterns over the area 21a. As usual, the dark and white strip-like patches exhibit activated and inactivated areas in the cortex, respectively. Qualitatively, there were several similarities observed in the patterns of orientation maps of areas 21a and 17. The equal-width dark patches were regularly separated by light patches of approximately identical width either in area 21a or in area 17. The "pinwheel" orientation centers (i.e., the focal points where all the orientations come together and the cortical cells respond to various orientations that radiate in a regular manner on the polar map of area 17) were also often observed on the polar orientation map of area 21a (shown later in Fig. 5A). Furthermore, like in area 17, the patterns of two maps (Figs. 2A and C or B and D)

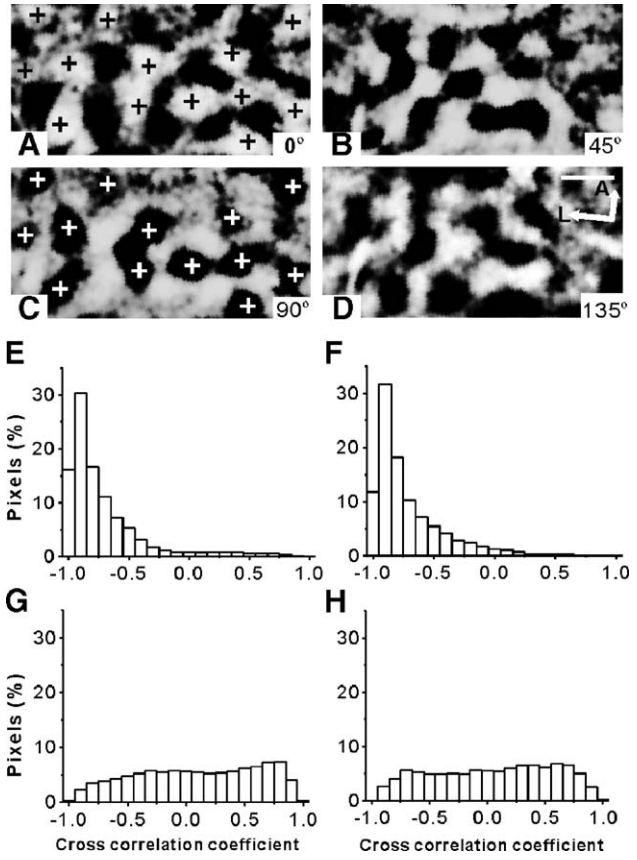

Fig. 2. Functional orientation maps of area 21a revealed by optical imaging and the similarity of their patterns. (A–D) Maps elicited by gratings oriented in horizontal (0°), vertical (90°) and diagonal (45° and 135°) meridians are shown in panels (A), (C), and (B) and (D) respectively. Scale bar: 1 mm in panel (D). A, anterior; L, lateral. (E)–(H) Histograms of cross correlation coefficients (CCCs) in panels (E), (F), (G) and (H) for maps (A) vs. (C), (B) vs. (D), (A) vs. (B), and (C) vs. (D), respectively. The mean CCCs were −0.72 and −0.71 for panels (E) and (F) respectively with peaks at −0.9 indicating that the patterns of two maps are spatially complementary. The mean CCCs were 0.091 and 0.043 in a flat distribution for panels (G) and (H) indicating the two patterns of maps A vs. B, or C vs. D differ completely.

in area 21a elicited by two orthogonal gratings were spatially complemented, as denoted by black and white crosses in Figs. 2A and C. To quantify the relationship of the two maps, the pixel vs. pixel cross-correlation coefficient (CCC) histograms are shown in Figs. 2E–H. In Figs. 2E and F, the distributions of the two CCC histograms were both peaked at −0.90 with mean CCCs of −0.72 and −0.71 for orientation map pairs of 0° and 90°, and 45°and 135°, respectively. This indicates that the two maps of each pair are spatially complementary. Notably, this spatial complementary relationship always remains in spite of the absolute orientation of stimulus gratings for any two maps of all 9 cats studied so long as the animal was stimulated with two gratings orthogonal each other. In contrast, the distributions of CCC histograms were rather flat with mean CCCs of 0.091 and 0.043 for map pairs of 0° and 45°, 90° and 135° (Figs. 2G and H) respectively, indicating almost no similarity between the two pairs of maps.

Quantitative measures revealed somewhat of differences in patterns of maps between areas 21a and 17. In all the experiments, the mean response strength (RS) of orientation maps of area 21a

($1.13 \pm 0.10 \times 10^{-4}$, hereinafter referred to as a mean ± SD, $n = 7$) was about 2.5 times weaker than that of area 17 ($2.88 \pm 0.14 \times 10^{-4}$, $n = 12$). The difference was statistically significant (t text, $P < 0.01$) indicating that the difference in responsiveness between the excited region and unexcited region to a given visual stimulus is remarkably weaker in area 21a than area 17. Furthermore, the mean width of the black and white patches randomly measured in the orientation map of area 21a (0.97 ± 0.12 mm, $n = 35$, in 6 cats) differed significantly from that in area 17 (1.04 ± 0.19 mm, $n = 50$, in 6 cats) (t test, $P < 0.05$). The ratio between the clock-wise and counter-clock-wise pinwheels in areas 21a and 17 was identical (0.934 (56/60) and 0.933 (110/118), respectively. Finally, the minimum distance between two neighboring pinwheel centers was also measured for each center in 6 cats. As a result of difference in patch width, their distribution histograms indicated that 57.8% of 129 pinwheel centers in area 21a had their minimum distance longer than 400 μm with a mean distance 455.47 ± 0.33 μm, while 68. 5% of 225 centers in area 17 had their minimum distance longer than 400 μm with a mean of 484.58 ± 0.25 μm (Fig. 3) showing a significant difference in functional organization between areas 21a and 17 (χ^2 test, $P < 0.05$). The mean density of pinwheel centers in area 21a (2.87 ± 0.37 per mm^2) was slightly higher than that of area 17 (2.29 ± 0.14 per mm^2) though the difference was not statistically significant between the two areas (t test, $P = 0.063 > 0.05$). Overall, these measures suggest that neurons' functional architecture in area 21a is more densely organized than in area 17.

Orientation columns in area 21a

To search the possible columnar organization throughout area 21a, we made a series of microelectrode penetrations orthogonal to the cortical surface to measure the responses of each successively recorded neuron to grating stimuli in 4 cats. It was found that the receptive fields of recorded neurons in area 21a are mostly concentrated in the central visual field in agree with previous reported (Tusa and Palmer, 1980; Updyke, 1986; Wimborne and Henry, 1992; Wang and Dreher, 1996; Wang et al., 2000). The preferred orientation of each cell encountered was obtained by calculating a vector sum of the cell's responses to a set of orientations of grating stimuli in the central visual field of the contralateral eye based on the circular statistics (see Methods, Batschelet, 1981; Zar, 1974). By this method, a preferred orientation vs. penetration distance curve was obtained for each penetration. Fig. 4 shows some typical examples of these experiments. Like cells in area 17, the preferred orientations of neurons along a vertical electrode penetration were similar in area 21a with few exceptions (Figs. 4C–G). The histological section, penetration reconstruction of an electrode track, and preferred orientations of neurons recorded along several penetrations were shown in Figs. 4A, B and C–G respectively. The preferred orientation differences of neighboring neurons (within 100 μm) in area 21a were less than 30° in 71% of all cell pairs tested and less than 15° in 50% of cell pairs (Fig. 4H), indicating a overall columnar clustering in orientation preference. Considering the significant curvature of area 21a, the relative difficulty in keeping an exactly orthogonal penetration and the identity of strip-like pattern on optical maps usually elicited by a constant stimulus at different depths (not shown here), we conclude that neurons with similar preferred orientations are arranged into slab-like columns which are orthogonal to the cortical surface of area 21a.

Oblique effect shown in orientation maps of area 21a

To get a functional map containing a set of orientations, 4 or 6 responses of optical signals at each pixel were obtained from a given cortex respectively when stimulated by 4 or 6 gratings of different orientations equally distributed from 0° to 180°. The preferred orientation and orientation bias were calculated for each pixel based on 4 or 6 values of luminance using vector summation and circular statistics. As a result of a complete set of 4 or 6 single-condition, color-coded polar maps were obtained pixel-by-pixel for areas 21a and 17 (Figs. 5A and C) Qualitatively, the two color-coded polar maps are quite similar. The regions of iso-preferred orientation were spatially continuous along the surface of the two imaged cortical areas. The "pinwheel" orientation centers were observed in area 21a (Figs. 5A and B), as well as in area 17 (Fig. 5C). Moreover, both cortical areas showed similar under-presentation of oblique meridians, qualitatively as seen in the two W-shape distribution histograms of preferred orientation, and the overrepresentation of horizontal and vertical meridians was more significant in area 21a (Fig. 5D) than that in area 17(Fig. 5E).

Quantitatively, the mean of relatively cortical areas (61.6 ± 2.2%) in which neurons responded preferentially to the horizontal (0°–22.5° and 157.5°–180°) and vertical meridians gratings (90° ± 22.5°) were very significantly larger than those (38.4 ± 2.3%) to the oblique (45° ± 22.5° and 135° ± 22.5°) in area 21a of 9 cats (t test, $P < 0.001$, $n = 9$) (Fig. 6A), while in area 17 of 14 cats, only

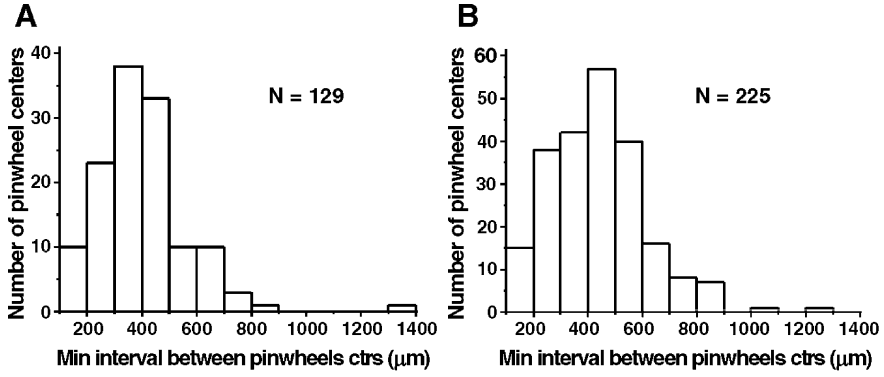

Fig. 3. Distribution histograms of the minimum intervals between pinwheel centers in areas 21a (A) and 17 (B). The minimum intervals longer than 400 μm in area 17 (68.5%) are more than that in area 21a (57.8%) suggesting a denser organization of orientation map in 21a compared with that in area 17. All the pinwheel centers intervals were measured from cortices of 6 cats.

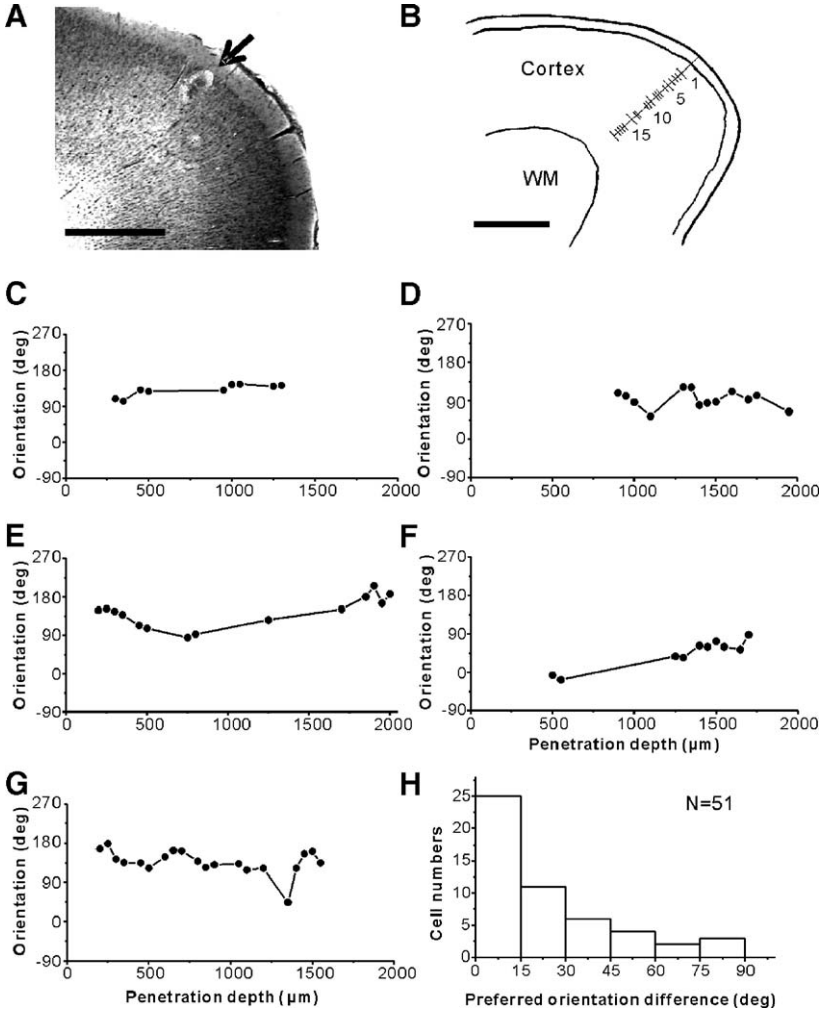

Fig. 4. Electrophysiological evidence of columnar organization of orientation preference in area 21a. (A) Photomicrograph of Nissl-stained coronal section through cortical area 21a indicating the hole of an electrode penetration with blood inside (denoted by an arrow). (B) Reconstruction of an electrode penetration through the cat's area 21a. The electrode was advanced along a direction vertical to the surface of the cortex. The positions of each units recorded along the penetration are indicated by the short lines numbered. The corresponding preferred orientations of neurons recorded along the same penetration in this cat are shown in panel G. WM, the white matter. Scale bars both in panels A and B: 1 mm. (C)–(F) Preferred orientations of cortical neurons recorded by electrodes along the 4 vertical penetrations in the cortex of two cats. (G) The preferred orientation of neurons recorded in an electrode track in area 21a of another cat, whose Nissl-stained section and penetration reconstruction are shown in panels A and B. Note that the most neurons encountered showed the roughly same preferred orientations with few exceptions, demonstrating that the columnar organization of orientation preference in area 21a similar to that which occurs in area 17. (H) Histogram of preferred orientation difference of neighboring neurons within 100 μm in area 21a. Note that the neighboring neurons had preferred orientation differences less than 15° in 50% cells tested and less than 30° in 71% cells. Data were from 4 cats tested.

52.6% and 47.4% of cortical area in average devoted to cardinal and oblique stimuli, respectively (t test, $P < 0.05$, $n = 14$) (Fig. 6B). The overrepresentation of horizontal and vertical preferences in area 21a (24.0 ± 3.9%, n = 9, Fig. 6A) was 4.6 times more than that in area 17 of the cat (5.2 ± 0.72%, $n = 14$, Fig. 6B). The difference is very significant (t test, $P < 0.0001$).

The response strengths of maps elicited by various gratings of orientations were also compared. Specifically, in area 21a of 7 cats tested, the mean response strength of orientation maps elicited by the horizontal and vertical gratings ($1.35 \pm 0.14 \times 10^{-4}$) was 1.4 times greater than those by the two diagonal gratings ($0.983 \pm 0.10 \times 10^{-4}$) showing a very significant difference (t test, $P < 0.005$, Fig. 6C). The response strength to either horizontal or vertical gratings was statistically higher than either of the two oblique stimuli (t test, all $P < 0.05$, Fig. 6C). In area 17 of 12 cats tested, the mean response strength to horizontal and vertical stimuli ($3.03 \pm 0.22 \times 10^{-4}$) was 1.1 times greater than those to oblique ones ($2.71 \pm 0.15 \times 10^{-4}$) ($t$ test, $P < 0.01$, Fig. 6D). However, only the response strength of the maps elicited by the vertical, but not horizontal grating, was statistically significant than either of the two oblique gratings (t test, both $P < 0.05$, Fig. 6D) showing a weaker oblique effect in response amplitude domain of area 17 than that of area 21a.

Discussion

Using optical imaging and single-unit electrophysiological recording methods, the present study provides the first evidence that the orientation selective neurons in higher order extrastriate cortical area 21a are organized in a slab-like columnar architecture in a large scale. The orientation columns on the map are more

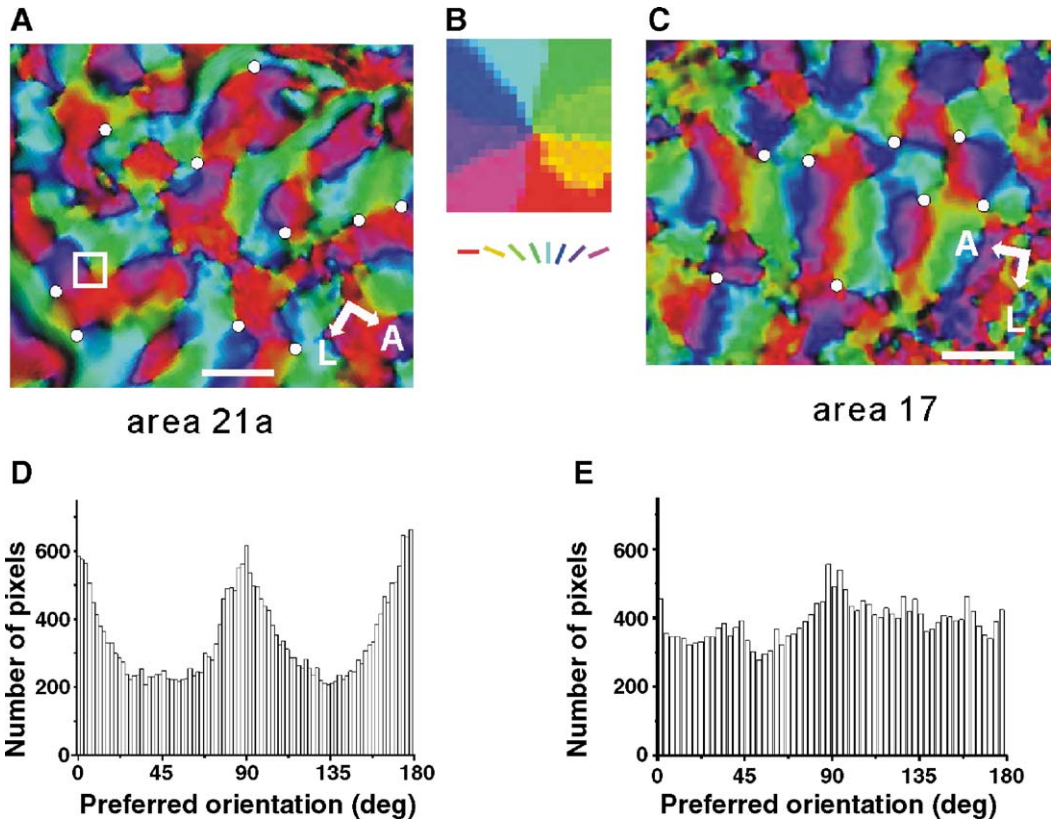

Fig. 5. Oblique effect revealed by optical imaging based on intrinsic signals in areas 21a and 17. (A) and (C) The two overall color-coded orientation polar maps showing functional organization of areas 21a (A) and 17 (C) in two cats, respectively. A complete set of 4 single-condition orientation maps were gathered and color-coded pixel-by-pixel on the two maps according to the color scale of orientations presented in the bottom of (B). The brightness indicates orientation bias of each pixel in the two polar maps. The orientation columns were spatially continuous along the surface of the imaged cortical areas. The preferred orientation was calculated for each pixel based on 4 values of orientation biases using vector summation. Several pinwheel points are shown clearly in both maps (denoted by white points in panels A, B and C). Scale bar: 1 mm in panels A and B. (B) A typical pinwheel center magnified from the small white square in panel A. (D) and (E) Preferred orientation histograms of the functional maps of areas 21a (D) and 17 (E), respectively. Note that both the histograms show a W-like distribution of preferred orientation with two peaks at horizontal (0° or 180°) and vertical (90°) meridians, suggesting that neurons prefer to respond to horizontal and vertical stimulus gratings more than those to diagonal, i.e., oblique effect. It is very clear that the effect observed in area 21a is much more significant then that in area 17.

densely distributed in area 21a than in area 17 of the cat. In area 21a, the orientation map substantially overrepresents horizontal and vertical contours showing a more significant neural oblique effect than that in area 17. Overall, our findings indicate that area 21a is a higher order cortex in charge of form information processing in the cat and may play an important role in visual perceptive process of the orientated contours.

Comparison of functions between areas 21a and 17

To our knowledge, no functional architecture in area 21a has been previously observed although there has been a concentrated effort of research on the response properties of area 21a neurons. Dreher et al. (1993) have shown that neighboring cells along an oblique penetration in area 21a tended to have variable preferred orientations. However, it is difficult to figure out the entire functional architecture in a large cortical area only using single-unit recording without a functional anatomical approach. Using optical imaging and single-unit recording, the current study clearly demonstrates a three-dimension slab-like architecture within area 21a and a spatially complementary distribution of orthogonal orientation columns as well.

The receptive field properties of area 21a neurons are similar to those of neurons in area 17 in many aspects (Dreher, 1986; Wimborne and Henry, 1992; Dreher et al., 1993; Tusa and Palmer, 1980; Wang et al., 2000; Wang and Dreher, 1996; Morley and Vickery, 1997). Our optical imaging and single-unit recording data also show that the receptive fields of neurons in area 21a are mostly concentrated in the central visual field in agreement with previous reports that most cells in area 21a have their receptive fields highly concentrated within a visuotopical eccentricity of 5° in the visual field and that they mainly receive feedforward input from and send feedback output to area 17 (Tusa and Palmer, 1980; Updyke, 1986; Wimborne and Henry, 1992; Dreher et al., 1993;Wang and Dreher, 1996, Wang et al., 2000). The observed similarity of these two cortical areas in functional architecture suggests that area 21a receives well-ordered retinotopic projection of area 17 in the central visual field.

The cells in extrastriate areas 18 and 19 are also organized into orientation columns (Hubel and Wiesel, 1965) and project to area 21a in the cat (Montero, 1981; Grant and Shipp, 1991; Sherk and Mulligan, 1993). The quantitative measures showing that the slab-like columnar architecture in area 21a is arranged more densely than in area 17 suggest that the highly convergent projections to

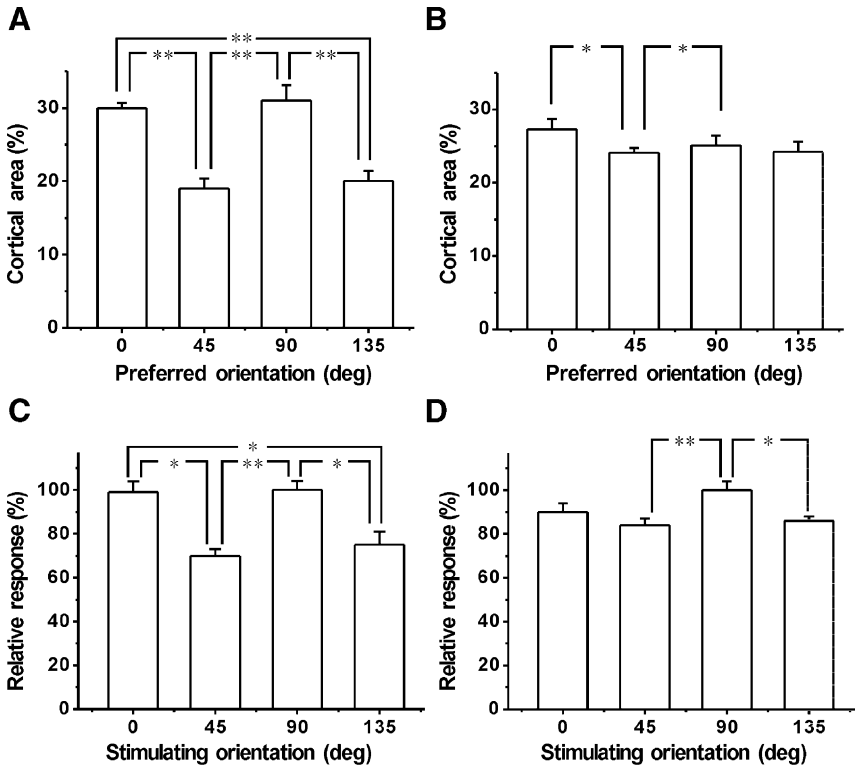

Fig. 6. Oblique effects in statistical measures in responsive area and response strength domains in areas 21a and 17. (A) and (B) Quantitative comparison of cortical areas in which cells preferred to respond to gratings of horizontal (0°–22.5° and 157.5°–180°), vertical (90° ± 22.5°) and two oblique orientations (45° ± 22.5°and 135° ± 22.5°) in areas 21a of 9 cats and area 17 of 14 cats, respectively. In paired t test, * represents $P < 0.05$; ** represents $P < 0.01$. The oblique effect in area 21a is more significant than in area 17. (C) and (D) Mean response strengths of 4 orientation maps elicited by differently oriented gratings of 0°, 45°, 90° and 135° in areas 21a of 7 cats showing the response strength to the horizontal or vertical gratings was statistically greater than to either of the two oblique. However, in area 17 of 12 cats, only the response strength to the vertical grating was greater than to an oblique. Therefore, in the response domain, neurons in area 21a also showed a more significant oblique effect than those in area 17.

area 21a from these multiple areas must be overlapped very precisely in the orientation domain.

Oblique effect in animals and human

The neural oblique effect is always referred to as more neurons in area 17 preferentially responding to horizontal and vertical contours than the oblique contours (Christopher et al., 2000; Mansfield, 1974; Albus, 1975; Maffei and Campbell, 1970; Shou et al., 1985; Yu and Shou, 2000; Leventhal and Hirsch, 1978; Wang et al., 2003). However, reports on oblique effect from different groups based on single-neuron recording showed discrepancies in counting cell numbers of different preferred orientations in the cortex (Mansfield, 1974; Leventhal and Hirsch, 1978; Albus, 1975). The discrepancy among these studies may be largely due to sampling problems that result from relatively limited numbers of electrode penetrations and different locations in the visual cortex. Furthermore, some functional magnetic resonance image (fMRI) and single-neuron recording studies failed to find a reliable neural oblique effect outside of V1 (V2, V3, VP) in human and animals (Christopher et al., 2000; Levitt et al., 1994). The failures may result from the weak fMRI response signals and also electrode sampling problems mentioned above, respectively. In contrast, the intrinsic signal optical imaging has the advantage of studying functional organization of the visual cortices, many of which are located on the hemispheric surface. This makes it possible to show the oblique effect in area 21a more significant than in area 17 even though the RS of area 21a is smaller than that of area 17. Recently, Wang et al. (2003) reported the neural oblique effect revealed by optical imaging in cat's area 18.

The qualitative similarity in the neural oblique effect further enhances the idea that areas 21a and 17 are mainly involved in form processing along the visual pathway in the cat. It is reported that about 7% overrepresentation area of cardinal contours than oblique contours in area 17 in developing and adult ferrets (Coppola et al., 1998a, b; Chapman and Bonhoeffer, 1998). Similar findings were also reported in area 17 of cats and human in electrophysiological, optical imaging, behavioral and fMRI studies (Yu and Shou, 2000; Shou et al., 1985; Maffei and Campbell, 1970; Bonds, 1982; Coppola et al., 1998a, b; Christopher et al., 2000). Neural oblique effect in area 21a is more significant than in area 17 presumably because neurons in area 21a mostly have their receptive fields in the central visual field.

The significance and neural origin of the oblique effect

The novel findings in area 21a here suggest a higher order extrastriate mechanism that may be involved in the superior perception of cardinal contours to which more neurons respond more strongly. The feedback projections from area 21a mainly appear to exert an excitatory influence on area 17 cells (Wang et al., 2000), which enhances the spatial frequency tuning of area 17 (Huang et al., 2004). The neural oblique effect in area 21a may reflect and in turn enhance the neural oblique effect in area 17

through feedback projections. The reciprocal excitation between areas 21a and 17 may play a role in generating perceptive oblique effect.

The function of area 21a in the cat has been suggested to relatively correspond to area V4 (or V3) in the monkey (Burke et al., 1998; Payne, 1993). An attention-induced enhancement in neurons' response was found in monkey areas V1 and V4 (McAdams and Maunsell, 1999). If the neural mechanism of the oblique effect in the cat is similar to that in the monkey it would be expected that like area 21a, the V4 might mediate the perception of psychological oblique effect in human because of the similarity of the visual cortex in primates and humans.

There has been anatomical and physiological evidence showing that more cells are distributed along the horizontal and vertical meridians than the oblique meridians in the retina (Stone, 1978; Hughes, 1981) and LGN (Vidyasagar and Urbas, 1982; Shou and Leventhal, 1989) indicating possible retinal and subcortical origins of the oblique effect. On the other hand, there is a radial distribution in dendritic fields (Leventhal and Schall, 1983) and physiologically preferred orientations of the retinal ganglion cells, the LGN and area 17 neurons (Levick and Thibos, 1982; Shou et al., 1986; Shou and Leventhal, 1989; Leventhal and Schall, 1983). This was also supported by a recent psychophysical study (Westheimer, 2003). The radial distribution of preferred orientations does not conflict with the neural oblique effect we found in area 21a with a retinotopic eccentricity less than 10°. In fact, most of LGN cells (Vidyasagar and Urbas, 1982; Shou and Leventhal, 1989) and simple cells in area 17 (Schall et al., 1986) subserving central vision exhibit horizontal and vertical orientations preferred although they also possess a radial distribution in the retina. The radial bias is strongest in retinal regions subserving the horizontal meridian (Schall et al., 1986; Shou and Leventhal, 1989).

Interestingly, the natural scenes all contain more horizontal and vertical contours than oblique contours (Coppola et al., 1998a, b), presumably due to the effect of gravity. Whether such a cardinal contour-dominant environment of the visual world contributes to the visual orientation anisotropy is of interest to study since the oblique effect seems to be innate (Leehey et al., 1975).

Acknowledgments

The study was supported by grants from the National Science Foundation of China (No.90208013), Ministry of Education of China and Chinese Academy of Sciences. Authors thank Dr. Chun Wang and Mr. Wei Shen for their helpful discussions on the manuscript; Mrs. Jason Clower and Bruce Hansen for reviewing and editing the manuscript.

References

Albus, K., 1975. A quantitative study of the projection area of the central and the paracentral visual field in area 17 of the cat: II. The spatial organization of the orientation domain. Exp. Brain Res. 24, 181–202.

Annis, R.C., Frost, B., 1973. Human visual ecology and orientation anisotropies in acuity. Science 182, 729–731.

Appelle, S., 1972. Perception and discrimination as a function of stimulus orientation: the "oblique effect" in man and animals. Psychol. Bull. 78, 266–278.

Batschelet, E., 1981. Circular Statistics in BiologyAcademic Press, New York, USA.

Bonds, A.B., 1982. An "oblique effect" in the visual evoked potential of the cat. Exp. Brain Res. 46, 151–154.

Burke, W., Dreher, B., Wang, C., 1998. Selective block of conduction in Y optical nerve fibres: significance for the concept of parallel processing. Eur. J. Neurosci. 10, 8–19.

Campbell, F.W., Kulikowski, J.J., Levinson, J., 1966. The effect of orientation on the visual resolution of gratings. J. Physiol. (London) 187, 427–436.

Chapman, B., Bonhoeffer, T., 1998. Overrepresentation of horizontal and vertical orientation preference in development ferret area 17. Proc. Natl. Acad. U. S. A. 95, 2609–2615.

Chen, X., Shou, T., 2003. Accurate establishment of the retinotopic topography of area 17 in cats by intrinsic signal optical imaging. Acta Physiol. Sin. 55, 541–546.

Chen, X., Sun, C., Huang, L., Shou, T., 2003. Selective loss of orientation column maps in visual cortex during brief elevation of intraocular pressure. Invest. Ophthalmol. Visual Sci. 44, 341–435.

Christopher, S., Furmanski, C.S., Engel, S.A., 2000. An oblique effect in human primary visual cortex. Nat. Neurosci. 3, 535–536.

Coppola, D.M., Purves, H.R., McCoy, A.N., Purves, D., 1998. The distribution of oriented contours in the real world. Proc. Natl. Acad. Sci. U. S. A. 95, 4002–4006.

Coppola, D.M., White, L.E., Fitzpatrick, D., Purves, D., 1998. Unequal representation of cardinal and oblique contours in ferret visual cortex. Proc. Natl. Acad. Sci. U. S. A. 95, 2621–2623.

Dreher, B., 1986. Thalamocortical and corticocortical interconnections in the cat visual system: relation to the mechanisms of information processing. In: Pettigrew, J.D., Sanderson, K.L., Levick, R.W. (Eds.), Visual Neuroscience. Cambridge Univ. Press, Cambridge, UK, pp. 290–314.

Dreher, B., Michalski, A., Ho, R.H.T., Lee, C.W.F., Burke, W., 1993. Processing of form and motion in area 21a of cat visual cortex. Vis. Neurosci. 10, 93–115.

Dreher, B., Wang, C., Turlejski, K.J., Djavadian, R.L., Burke, W., 1996. Areas PMLS and 21a of cat visual cortex: two functionally distinct areas. Cereb. Cortex 6, 585–599.

Dreher, B., Djavadian, R.L., Turleiski, K.J., Wang, C., 1966. Areas PMLS and 21a of cat visual cortex are not only functionally but also hodologically distinct. Prog. Brain Res, 112, 251–276.

Furmanski, C.S., Engel, S.A., 2000. An oblique effect in human primary visual cortex. Nat. Neurosci. 3, 535–536.

Godecke, I., Bonhoeffer, T., 1996. Development of identical orientation maps for two eyes without common visual experience. Nature 379, 251–254.

Grant, S., Shipp, S., 1991. Visuotopic organization of the lateral suprasylvian area and an adjacent area of the ectosylvian gyrus of cat cortex: a physiological and connectional study. Vis. Neurosci. 6, 315–338.

Howard, I.P., 1982. Human Visual OrientationWiley Press, New York, USA.

Huang, L., Chen, X., Shou, T., 2004. Spatial frequency-dependent feedback of visual cortical area 21a modulating functional orientation column maps in areas 17 and 18 of the cat. Brain Res. 998, 194–201.

Hubel, D.H., Wiesel, T.N., 1962. Receptive fields, binocular interaction and functional architecture in the cat's visual cortex. J. Physiol. 160, 106–154.

Hubel, D.H., Wiesel, T.N., 1965. Receptive fields and functional architecture in two non-striate visual areas (18 and 19) of the cat. J. Neurophysiol. 28, 229–289.

Hubel, D.H., Wiesel, T.N., 1974. Sequence regularity and geometry of orientation columns in the monkey striate cortex. J. Comp. Neurol. 158, 267–294.

Hughes, A., 1981. Population magnitudes and distribution of the major modal class of cat retinal ganglion cells as estimated from HRP filling and a systematic survey of the soma diameter spectra for classical neurons. J. Comp. Neurol. 197, 303–339.

Leehey, S.C., Moskowitz-Cook, A., Brill, S., Held, R., 1975. Orientational anisotropy in infant vision. Science 190, 900–902.

Leventhal, A.G., Hirsch, H.V.B., 1978. Receptive-field properties of neurons in different laminae of visual cortex of the cat. J. Neurophysiol. 41, 948–962.

Leventhal, A.G., Schall, J.D., 1983. Structural basis of orientation sensitivity of cat retinal ganglion cells. J. Comp. Neurol. 220, 465–475.

Levick, W.R., Thibos, L.N., 1982. Analysis of orientation bias in cat retina. J. Physiol. 329, 243–261.

Levitt, J.B., Kiper, D.C., Movshon, J.A., 1994. Receptive fields and functional architecture of macaque V2. J. Neurophysiol. 71, 2517–2542.

Maffei, L., Campbell, F.W., 1970. Neurophysiological location of the vertical and horizontal visual coordinates in man. Science 167, 386–387.

Mansfield, R.J., 1974. Neural basis of orientation perception in primate vision. Science 186, 1133–1135.

McAdams, C.J., Maunsell, J.H.R., 1999. Effects of attention on orientation-tuning functions of single neurons in macaque cortical area V4. J. Neurosci. 19, 431–441.

Michalski, A., Wimborne, B.M., Henry, G.H., 1993. The effect of reversible cooling of cat's primary visual cortex on the responses of area 21a neurons. J. Physiol. 466, 133–156.

Montero, V.M., 1981. Comparative studies on the visual cortex. In: Woolsey, N. (Ed.), Cortical Sensory Organization, Multiple Visual Areas, Vol. 2. Humana Press, Clifton, NJ, USA, pp. 33–81.

Morley, J.W., Vickery, R.M., 1997. Spatial and temporal frequency selectivity of cells in area 21a of the cat. J. Physiol. (London) 501, 405–413.

Moveshon, J.A., Thompson, I.D., Tothurst, D.J., 1978. Spatial and temporal contrast sensitivity of neurons in areas 17 and 18 of the cat's visual cortex. J. Physiol. 283, 101–120.

Palmer, L.A., Rosenquist, A.C., Tusa, R.J., 1978. The retinotopic organization of lateral suprasylvian visual areas in the cat. J. Comp. Neurol. 177, 237–256.

Payne, B.R., 1993. Evidence for visual cortical area homologs in cat and macaque monkey. Cereb. Cortex 3, 1–25.

Rosenquist, A.C., 1985. Connections of visual cortical areas in the cat. In: Peters, A., Jones, E.G. (Eds.), Cerebral Cortex, Visual Cortex, Vol. 3. Plenum Press, New York, USA, pp. 81–116.

Retzlaff, H.E., Grinvald, A., 1991. A tandem-lens epifluorescence macroscope: hundred-fold brightness advantage for wide-field imaging. J. Neurosci. Methods 36, 127–137.

Schall, J., Vitek, D.J., Leventhal, A.G., 1986. Retinal constraints on orientation specificity in cat visual cortex. J. Neurosci. 6, 823–836.

Sherk, H., Mulligan, K.A., 1993. A reassessment of the lower visual field map in striate-recipient lateral suprasylvian cortex. Vis. Neurosci. 10, 131–158.

Shou, T., Leventhal, A.G., 1989. Organized arrangement of orientation-sensitive relay cells in the cat's dorsal lateral geniculate nucleus. J. Neurosci. 9, 4287–4302.

Shou, T-D., He, Z-J., Yu, M-Z., Zhou, Y-F., 1985. Different orientation effect of visual evoked potential due to different temporal stimulating frequency. Acta Physiol. Sin. 37, 199–203 (in Chinese).

Shou, T., Ruan, D., Zhou, Y., 1986. The orientation bias of LGN neurons shows topographic relation to area centralis in the cat retina. Exp. Brain Res. 64, 233–236.

Stone, J., 1978. The number and distribution of ganglion cells in the cat's retina. J. Comp. Neurol. 180, 753–772.

Thibos, L.N., Levick, W.R., 1985. Orientation bias of brisk-transient Y-cells of the cat retina for drifting and alternating gratings. Exp. Brain Res. 58, 1–10.

Timmney, B.N., Muir, D.W., 1976. Orientation anisotropy: Incidence and magnitude in Gaucasian and Chinese subjects. Science 193, 699–701.

Tusa, R.J., Palmer, L.A., 1980. Retinotopic organization of areas 20 and 21 in the cat. J. Comp. Neurol. 193, 147–164.

Tusa, R.J., Palmer, L.A., Rosenquist, A.C., 1978. The retinotopic organization of area 17 striate cortex in the cat. J. Comp. Neurol. 177, 213–235.

Tusa, A.J., Palmer, L.A., Rosenquist, A.C., 1981. Multiple cortical visual areas: visual field topography in the cat. In: Woolsey, C.N. (Ed.), Cortical Sensory Organization, Multiple Visual Aareas, vol. 2. Humana.Press, Clifton, NJ, USA, pp. 1–31.

Updyke, B.V., 1986. Retinotopic organization within the cat's posterior suprasylvian sulcus and gyrus. J. Comp. Neurol. 246, 265–280.

Vidyasagar, T.R., Urbas, J.V., 1982. Orientation sensitivity of cat LGN neurons with and without inputs from visual cortical areas 17, 18. Exp. Brain Res. 46, 272–277.

Wang, C., Dreher, B., 1996. Binocular interactions and disparity coding in area 21a of cat extrastriate visual cortex. Exp. Brain Res. 108, 257–272.

Wang, C., Waleszczyk, W.J., Burke, W., Dreher, B., 2000. Modulatory influence of feedback projections from area 21a on neuronal activities in striate cortex of the cat. Cereb. Cortex 10, 1217–1232.

Wang, G., Ding, S., Yunokuchi, K., 2003. Difference in the representation of cardinal and oblique contours in cat visual cortex. Neurosci. Lett. 338, 77–81.

Westheimer, G., 2003. The distribution of preferred orientations in the peripheral visual field. Vision Res. 43, 53–57.

Wimborne, B.M., Henry, G.H., 1992. Response characteristics of the cells of cortical area 21a of the cat with special reference to orientation specificity. J. Physiol. (London) 449, 457–478.

Wörgötter, F., Eysel, U.T., 1987. Quantitative determination of orientational and directional components in the response of visual cortical cells to moving stimuli. Biol. Cybern. 57, 349–355.

Wörgötter, F., Grundel, O., Eysel, U.T., 1990. Quantification and comparison of cell properties in cat's striate cortex determined by different types of stimuli. Eur. J. Neurosci. 2, 2928–2941.

Yu, H., Shou, T., 2000. The oblique effect revealed by optical imaging in primary visual cortex of cats.. Acta Physiol. Sin. 52, 431–434 (in Chinese).

Zar, J.H., 1974. Circular Distributions. Biostatistical AnalysisPrentice-Hall Press, Englewood Cliffs, NJ, USA.

Zhan, X., Shou, T., 2002. Anatomical evidence of subcortical contributions to the orientation selectivity and columns of the cat's primary visual cortex. Neurosci. Lett. 324, 247–251.